Terrestrial Organic Carbon Inputs to Marine Sediments

Reading List

•Prahl F.G., Ertel J.R., Goni M.A., Sparrow M.A. and Eversmeyer B. (1994) Terrestrial organic contributions to sediments on the Washington margin.*Geochim. Cosmochim. Acta* **58**, 3035-3048.

• Goni M.A., Ruttenberg K.C. and Eglinton T.I. (1997) Sources and contribution of terrigenous organic carbon to surface sediments in the Gulf of Mexico. *Nature*, **389**, 275-278.

• Hedges J.I., Keil R.G. and Benner R. (1997) What happens to terrestrial organic matter in the ocean? *Org. Geochem*. **27**, 195-212.

• Hedges J.I. and Oades J.M. (1997) Comparative organic geochemistries of soils and marine sediments. *Org. Geochem*. **27**, 319-361.

• Leithold & Blair (2001) Watershed control on the carbon loading of marine sedimentary particles. GCA 65, 2231-2240.

• Goni et al. (2005) The supply and preservation of ancient and modern components of organic carbon in the Canadian Beaufort Shelf of the Arctic Ocean. Mar. Chem. 93, 53-73.

• Schefuss et al. 2003 Carbon isotope analyses of *n*-alkanes in dust from the lower atmosphere over the central eastern Atlantic. GCA 67, 1757-1767.

Significance of Terrestrial Organic Carbon

- Most (ca. 90%) of the OC burial in present-day marine sediments occurs on continental margins and in deltas.
- Because they lie at the land-ocean interface, these depositional environments have the potential to be strongly influenced by terrestrial organic carbon inputs.
- The flux of POC from land is sufficient to account for all the OC being buried in marine sediments.
- Terrestrial OM is relatively poor in N relative to marine OM, and hence might be expected to be less susceptible to (re)cycling (reduced respiration) and preferentially accumulate in marine OC reservoirs.
- This doesn't appear to be the case, so what happens to terrestrial OC?

Implications:

- Global carbon budgets
- Long-term controls on atmospheric CO_2 and O_2.
- Estimates of export of primary production from surface ocean.
- Inferences of past productivity in the oceans from OC-based sediment records.
- Interpretation of records of terrestrial and marine productivity from marine sediments.

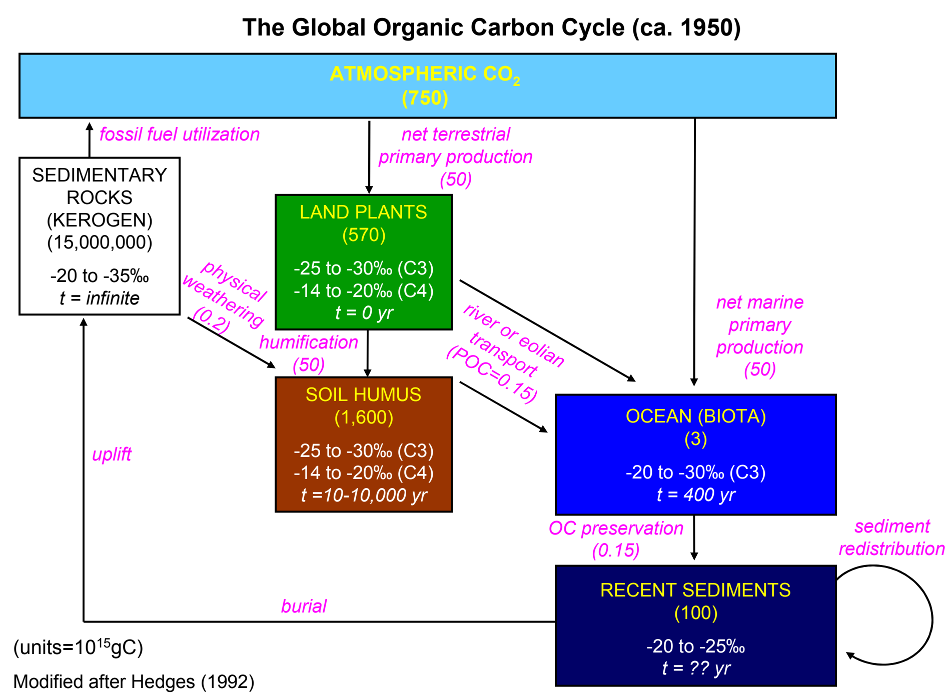

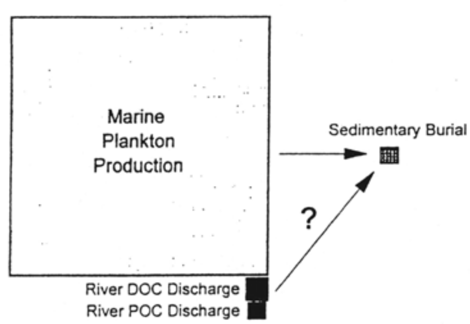

Fig. 2. Relative magnitudes of inputs and sinks of organic carbon to the ocean (from Hedges and Oades, in press). For scale, the areas illustrated for net marine plankton production and for sedimentary burial are 50 and 0.15 Gt C yr^{-1}, respectively. The respiration flux (not shown) is essentially equivalent to plankton production.

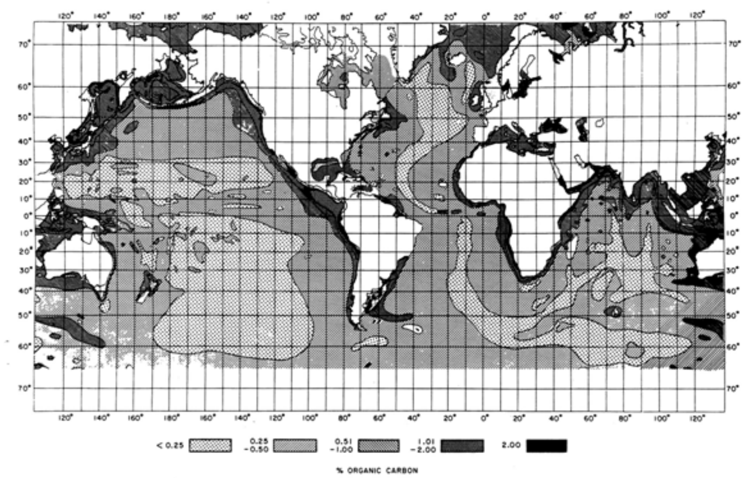

Organic carbon burial in marine sediments

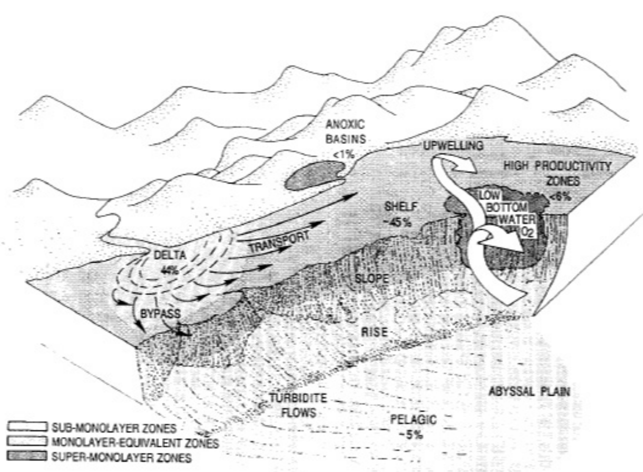

Fig. 1. Idealized diagram depicting current estimates of the percentage of total organic matter burial occurring within various marine sediment types (see Table 2). Light sections represent sediments which contain organic loadings lowe yr than a monolayer equivalent. Stippled sediments contain monolayer-equivalent loadings, and dark sediments contain loadings that are more than monolayer-equivalent.

Important Considerations

- Organic compounds synthesized by organisms are subject to biological and physicochemical processes that alter their chemical composition, and complicate their recognition and quantification in downstream organic carbon (OC) reservoirs such as soils and sediments.
- This “pre-conditioning” that modifies organic matter prior to burial may influence its reactivity in the sub-surface (e.g., by physical association or chemical reaction).
- The time-scales over which organic matter is processed prior to burial may also vary substantially, depending on its origin.
- As a result, contemporaneously deposited organic material of terrestrial and marine origin may exhibit a range of ages and labilities.
- In seeking to quantify the proportions of organic matter preserved in the sub-surface that stem from different sources it is important to find tracer properties that are largely independent of degradation.
- Continental margins contain significant quantities of “pre-aged” organic carbon.

Approaches to quantify OC inputs to marine sediments

- *Bulk parameters*
- - $C_{organic}/N_{total}$
- - $\delta^{13}C_{TOC}$

- *Molecular parameters*
- - Regression of terrestrial biomarker concentrations vs bulk properties ($\delta^{13}C$, C_{org}/N)
- extrapolation to zero marker concentration yields a bulk marine end-member elemental or isotopic value that can be inserted into isotopic/elemental mass balance.
- - Direct use of concentration measurements for biomarkers in “representative” end-member samples (e.g. plant wax biomarkers in riverine suspended sediments) to determine extent of dilution by marine OC.

Limitations:

- Typically, only 2 end-members are considered (marine and vascular plant), and terrestrial end-member biased towards vascular plant inputs.
- Constancy in composition is assumed along transects.

Bulk properties used to quantify terrestrial OC inputs

C_{org}./N ratios

- Principle: Vascular plant biomass is depleted in nitrogen (mainly comprised of cellulose and lignin), compared to [protein-rich] marine phytoplankton.
- Limitations:
- - Diagenetic influences - proteins are relatively labile, resulting in increased C_{org}/N ratios with degradation.
- Inorganic N bound in clays can affect ratio, especially in low TOC sediments.

δ^{13}C OC composition

- Principle: OC from marine primary production typically enriched in ^{13}C relative to C_3 vascular plant carbon.
- Limitations:
- Complications due to mixed inputs of C_3 and C_4 higher plant carbon.
- Past and present-day variations in δ^{13}C value of marine end-member.
- Potential diagenetic influences due to intermolecular isotopic variations (e.g. selective preservation of ^{13}C-depleted lipids over ^{13}C-enriched proteins)

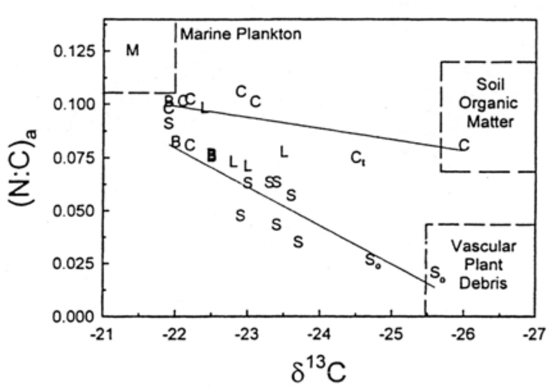

Fig. 5. Atomic N/C ratio versus stable carbon isotopic composition (δ^{13}C, ‰) of organic matter in size and density fractions isolated from Washington coast sediments (Keil *et al.*, 1994). M is marine material, B is bulk sediment, C is clay-, L is silt- and S is sand-sized sediment. Subscript t is high density ($\rho > 2.6$) fraction and subscript o is low density ($\rho < 1.5$) fraction.

%$C_{organic}$ and %N_{total} in surface marine sediments (Gulf of Mexico)

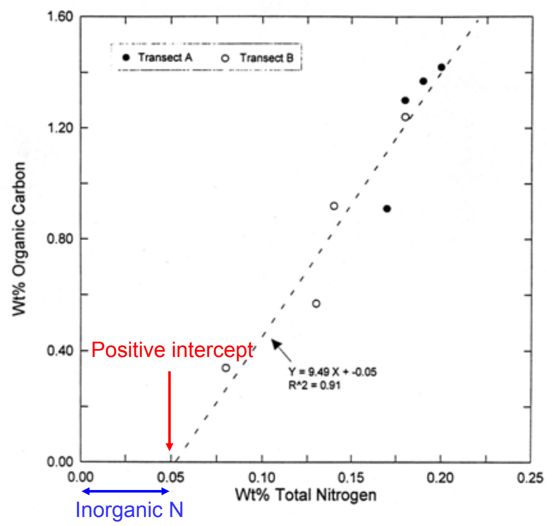

%OC vs specific mineral surface area for river (solid symbols) and delta (open symbols) sediments.

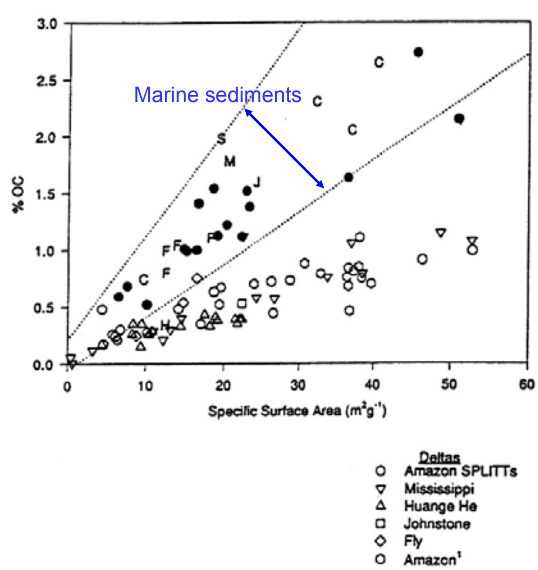

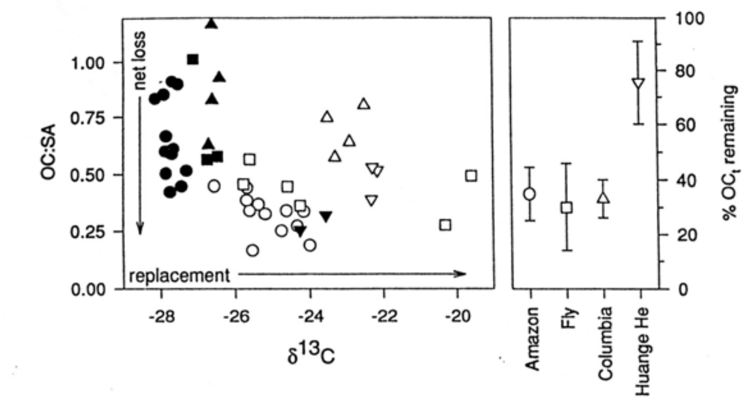

Fig. 2. Organic carbon to mineral surface area ratio (OC:SA) plotted against organic matter stable carbon isotope composition. River samples are as filled and delta samples are as open symbols. A shift downward in OC:SA denotes net loss of organic matter in the sediment mineral fractions, and a shift toward more positive isotopic compositions indicates addition of marine organic matter. The right hand side of the figure illustrates the average (±1 std) total amount of terrestrial organic matter (OC_t) remaining in deltaic sediments after accounting for both shifts in OC:SA and $\delta^{13}C$ between river and delta sediments for the coupled river-delta systems studied to date.

Biological markers as tracers of terrestrial OC inputs

Compound types

- \- Plant waxes (long-chain *n*-alkanes, *n*-alcohols, *n*-alkanoic acids)
- \- Terpenoids (e.g., abietic acid, retene, taraxerol)
- \- branched ether lipids
- \- Lignin phenols
- \- Cutin
- \- Tannins, Suberins

Molecular markers of terrestrial vegetation

Two primary groups of compounds have been used to trace present and past terrestrial (vascular plant) vegetation inputs in aquatic sediments:

Higher plant epicuticular leaf waxes:

n-alkanes
n-alkanoic acids
n-alkanols

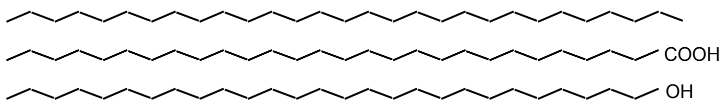

Lignin-derived phenols:

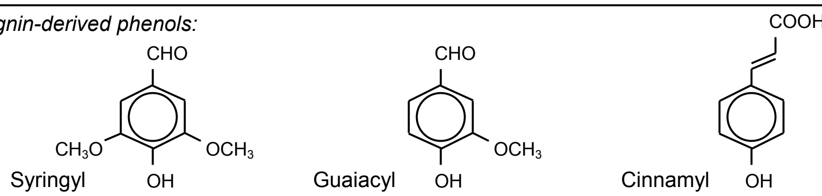

Lignin-derived phenols from CuO oxidation

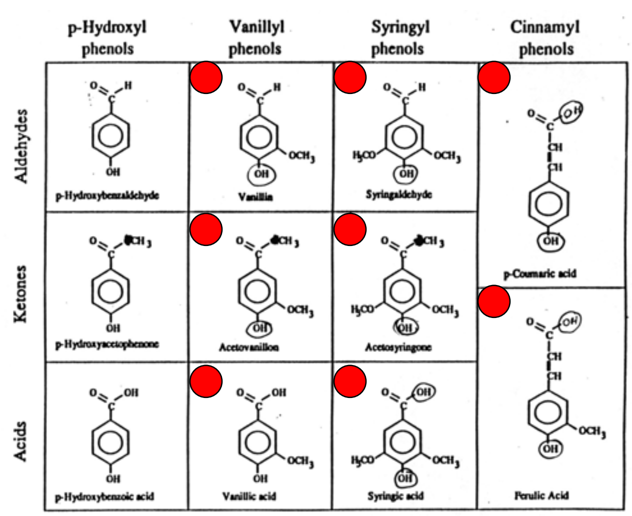

Used in determination of Lamda-8

Molecular markers of terrestrial vegetation

Lignin Compositional Parameters

Lignin-derived phenols

- syringyl/guaiacyl ratio (S/V): angiosperm vs. gymnosperms
- cinnamyl/guaiacyl ratio (C/V): leafy vs woody vegetation
- acid/aldehyde ratio (Ad/Al)v: extent of lignin degradation
- $\delta^{13}C$: Determination of C3 vs C4 vs CAM inputs

Compositional parameters derived from CuO oxidation products

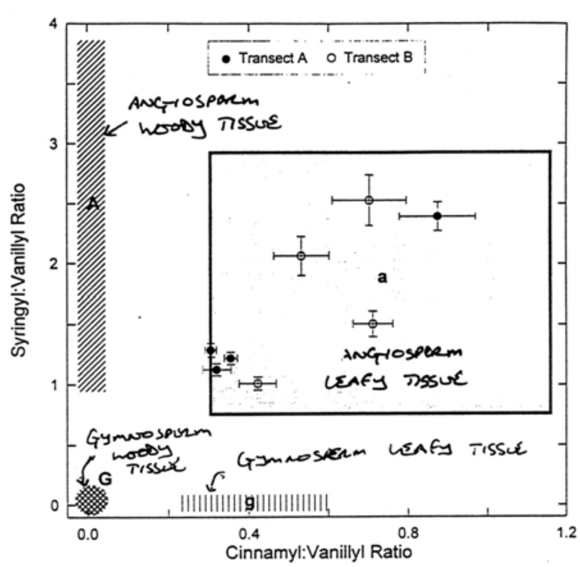

Stable carbon isotopic analysis of lignin-derived phenols

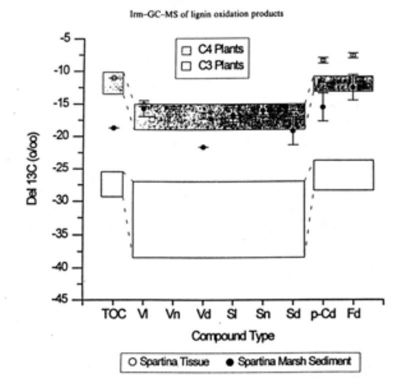

Fig. 4. Plot of $\delta^{13}C$ of TOC and individual lignin CuO oxidation products of organic matter concentrates from living *Spartina alterniflora* tissue (open symbols) and *Spartina* marsh sediment (closed symbols). Error bars represent ± one standard deviation from average $\delta^{13}C$ (‰). Included are areas representing the compositional ranges of C_3 and C_4 plant tissues (Table 4).

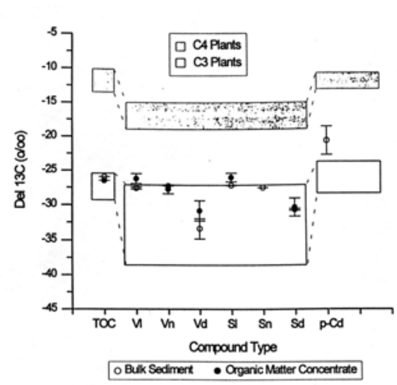

Fig. 6. Plot of $\delta^{13}C$ of TOC and individual lignin CuO oxidation products of bulk sediments (open symbols) and sedimentary organic matter concentrate (closed symbols) from Lake Washington. Error bars represent ± one standard deviation from average $\delta^{13}C$ (‰). Included are shaded areas representing the compositional ranges of C_3 and C_4 plant tissues analyzed (Table 4).

Epicuticular waxes on corn leaf surface

Waxes on leaf surface (white)

Leaf stomata

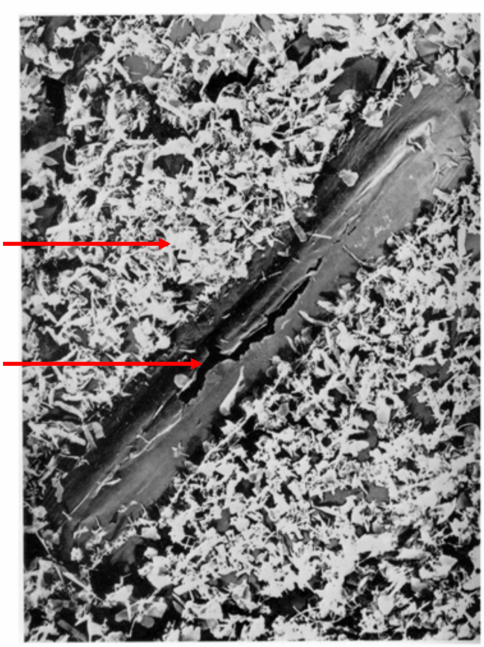

Example gas chromatogram of waxes (alkane fraction) from Tobacco leaves

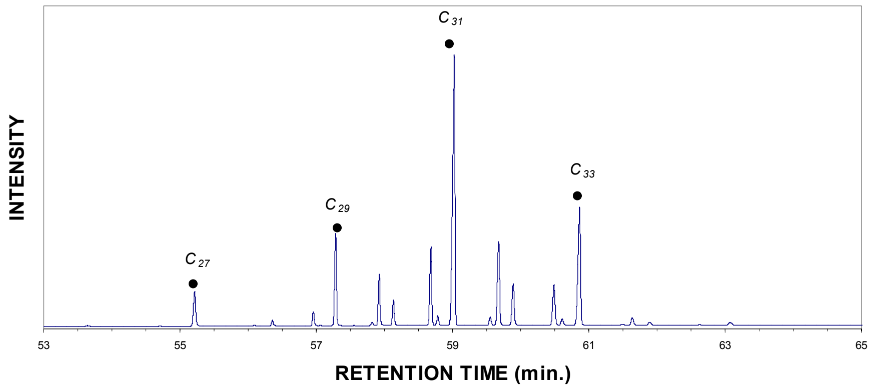

This figure shows a typical gas chromatography trace of a hydrocarbon (alkane) fraction extracted and purified from a higher plant leaf sample. Note the predominance of long-chain (>C_{24}) odd-carbon-numbered *n*-alkanes (marked with circles) that is highly characteristic of higher plant leaf waxes. The chain-length distribution of these compounds is indicative of growth temperature.

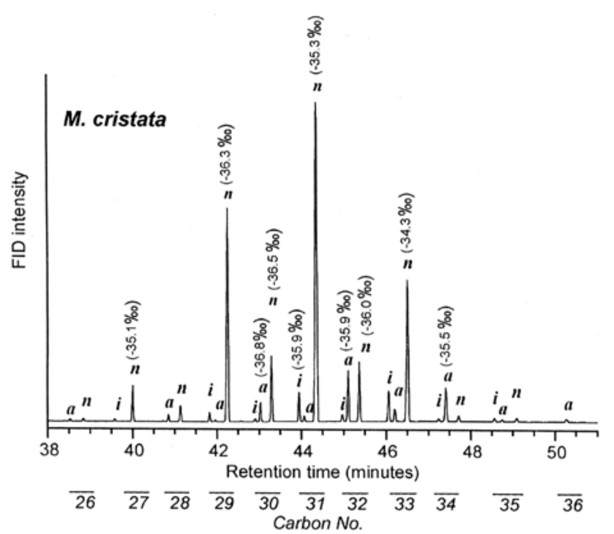

Fig. 1. Gas chromatogram of the *M. cristata* extract. *Anteiso-*, *iso-* and *n*-alkanes are labeled with *a*, *i* and *n*, respectively. $\delta^{13}C$ values for each compound are listed in parentheses.

Molecular markers of terrestrial vegetation

Plant Wax Compositional Parameters

Plant wax n-alkanes/n-alcohols/n-acids

- Carbon Preference Index (CPI) or Odd-over-Even Predominance (OEP)
  $CPI = 2\Sigma odd\ C_{21}\text{-to-}C_{35}/(\Sigma even\ C_{20}\text{-to-}C_{34} + \Sigma even\ C_{22}\text{-to-}C_{36})$

- Average chain length (ACL)
  $ACL = (\Sigma[C_i] \times i)/\Sigma[C_i]$ where:
  i is the range of carbon numbers (typically 23-35 for alkanes)
  C_i is the relative concentration of the alkane containing i carbon atoms.

- $\delta^{13}C$: Determination of C3 vs C4 vs CAM inputs

- δD: aridity/water stress

The Columbia River/Washington margin system

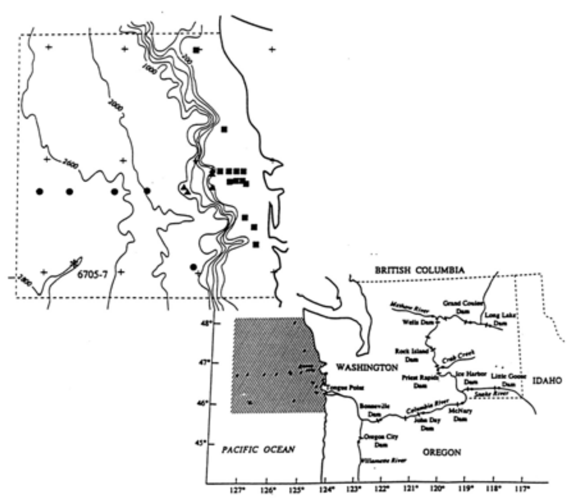

FIG. 1. Map identifies fourteen sampling locations behind major dam sites within the Columbia River drainage basin. The cross-hatched area and corresponding inset indicates twenty-three offshore sites on the Washington margin also examined in this study. The specific coordinates of shelf (filled squares), slope (filled triangles), and Cascadia Basin (filled circles) sampling locations are given in Table 1. The location for gravity core 6705-7 collected from the Cascadia Seachannel on the Astoria Fan (2688 m water depth: 46°03.6'N 126°37.9'W) is identified by the asterisk.

Higher plant biomarkers in Washington Margin sediments

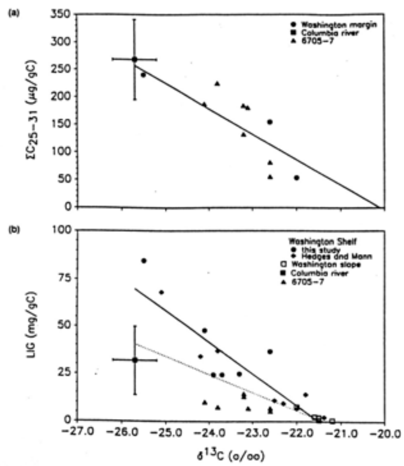

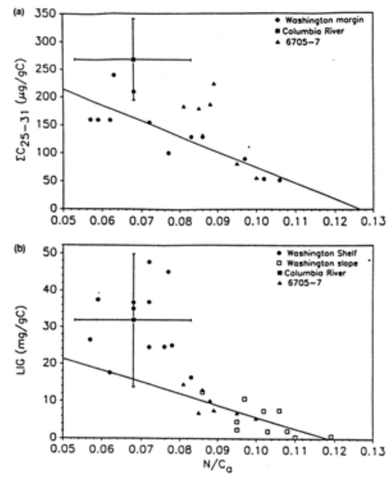

Prahl et al. 2004

Lignin phenol contents and isotopic compositions of Gulf of Mexico sediments

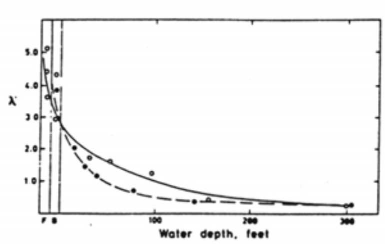

Fig. 4. Plots of λ against water depth at the sampling site for sediments from the Atchafalaya River and Terrebonne Bay transects. Open circles and solid line correspond to the Terrebonne Bay transect. Solid circles and dashed line correspond to the Atchafalaya Bay transect. Abbreviations: F, freshwater or brackish water sediments; B, bay sediments.

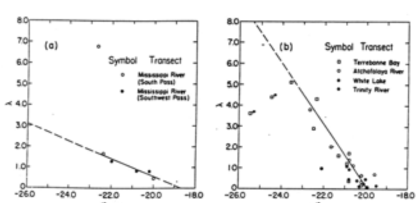

Fig. 5. Plots of λ against $\delta^{13}C$ for sediments from the (a) Mississippi River and (b) northwest Gulf depositional zones. Correlation lines were determined as the best least-squares fit to a straight line. Freshwater swamp sediments from the Terrebonne Bay transect are denoted in (b) by an asterisk and were not used to determine the correlation line. Southwest Pass sample no. 1 was not used to determine the Mississippi River correlation line.

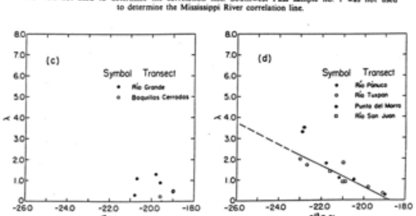

Fig. 6. Plots of λ against $\delta^{13}C$ for sediments from (c) the Rio Grande and (d) the southwest Gulf depositional zones. Punta del Morro sample no. 1 (*) contained large fragments of gymnosperm wood and, therefore, was not used to determine the correlation line in (d).

Hedges and Parker, 1976

Evidence for minimal terrestrial OC contributions to marine sediments

- Variations in OC:SA and $\delta^{13}C_{OC}$ in estuaries.
- Low C_{org}/N values for marine sediments.
- Enriched $\delta^{13}C$ values of marine sedimentary OC relative to terrestrial (C_3 OC).
- Rapid decrease in lignin phenols with distance offshore.

Evidence for significant terrestrial OC contributions to marine sediments

- Unknown contributions from ^{13}C-enriched (C_4) terrestrial OC sources.
- Importance of hydrodynamic processes in exporting terrestrial OC.
- Old core-top ages for continental margin sediments.
- Global influence of small, mountainous rivers.
- Arctic ocean undersampled.
- Widespread distribution of plant wax lipids in ocean sediments.
- Greater importance of terrestrial OC in glacial times (low sea-level stand)?

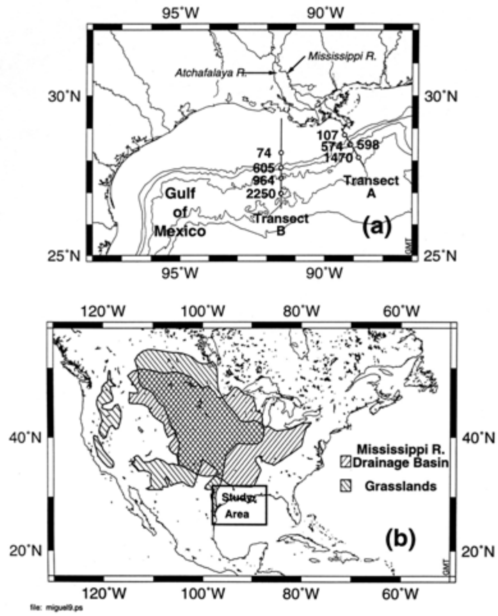

Compositional and Isotopic analyses of Gulf of Mexico sediments

Compositional & Isotopic analyses of Gulf of Mexico sediments

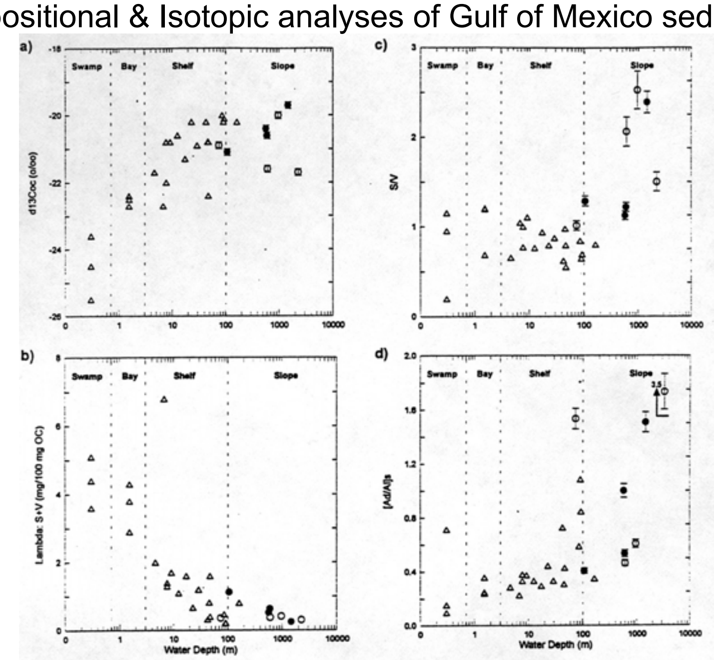

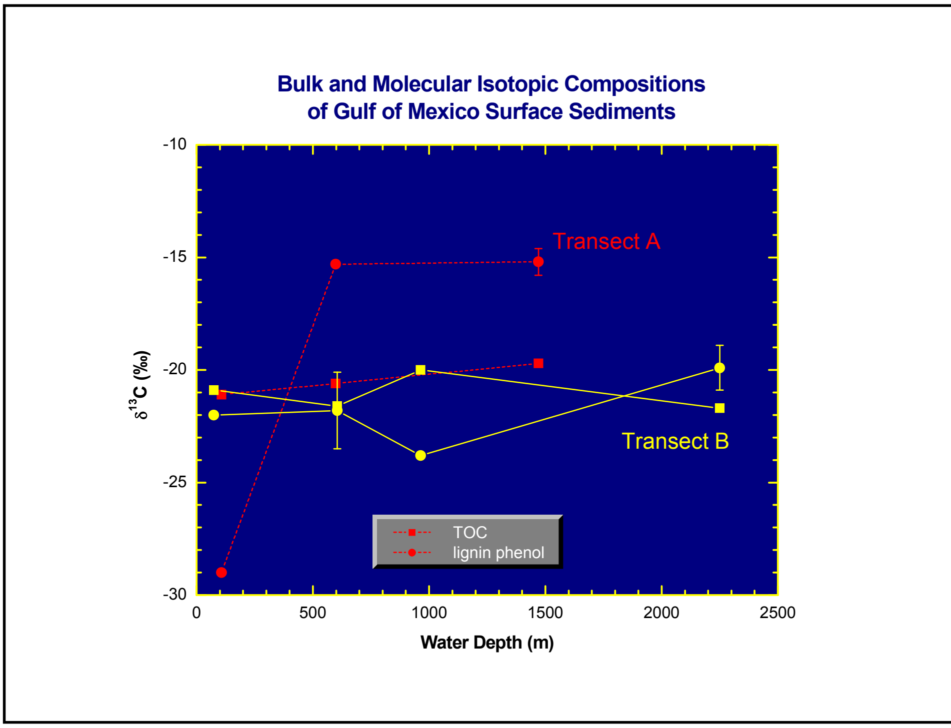

Bulk and Molecular Isotopic Compositions
of Gulf of Mexico Surface Sediments
-10
-15
-20
-25
-30
$\delta^{13}C$ (‰)
0
500
1000
1500
2000
2500
Water Depth (m)
Transect A
Transect B
TOC
lignin phenol

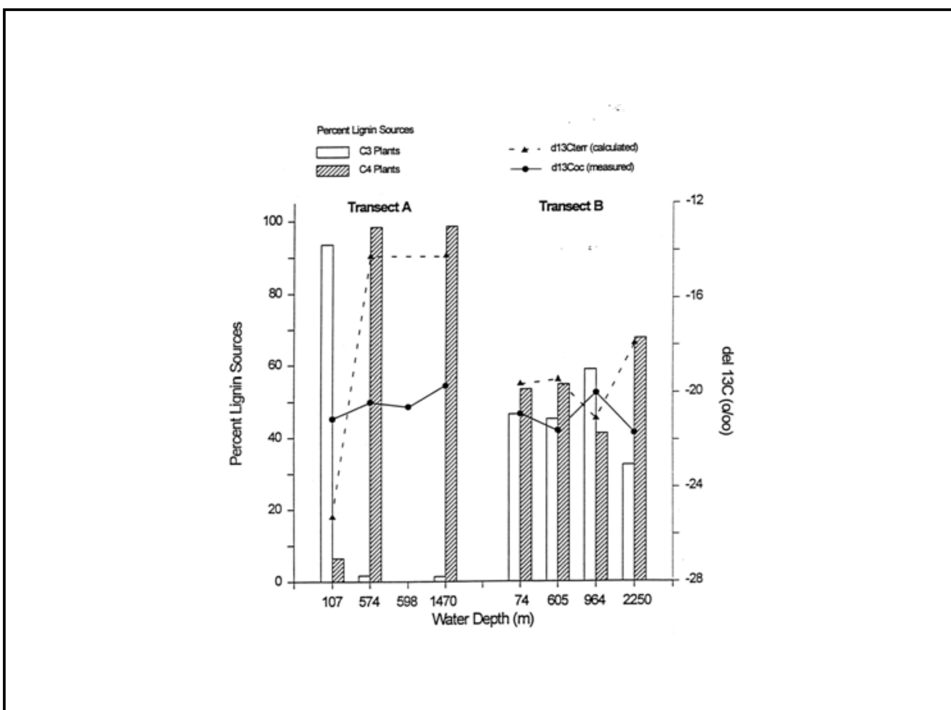

Percent Lignin Sources
C3 Plants
C4 Plants
d13Cterr (calculated)
d13Coc (measured)
Transect A
Transect B
100
80
60
40
20
0
Percent Lignin Sources
-12
-16
-20
-24
-28
del 13C (o/oo)
107
574
598
1470
74
605
964
2250
Water Depth (m)

Stable carbon isotopic characteristics of riverine SPOM

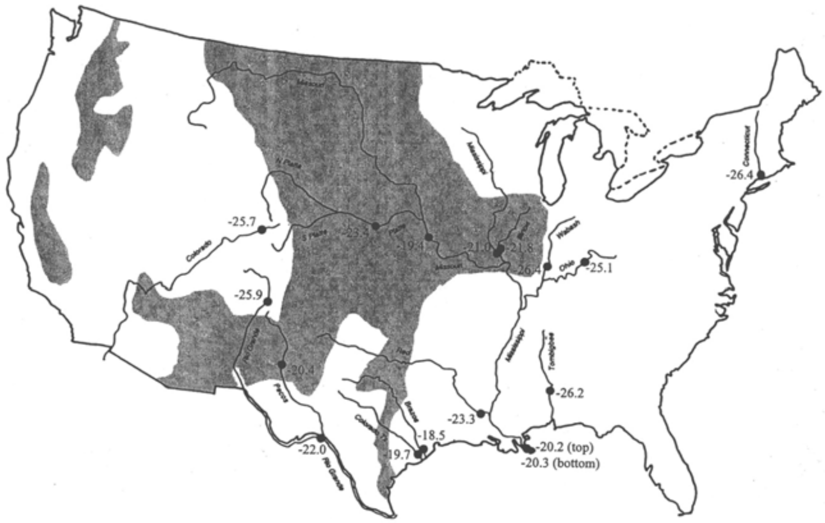

Fig. 1. Map of the continental United States with river sample sites (Canfield, 1997), and $\delta^{13}C$ values of suspended POM from those sites, illustrated. The distribution of C4 grasslands (shaded area) is adapted from Coupland (1979).

Carbon isotopic compositions of leaf wax biomarkers

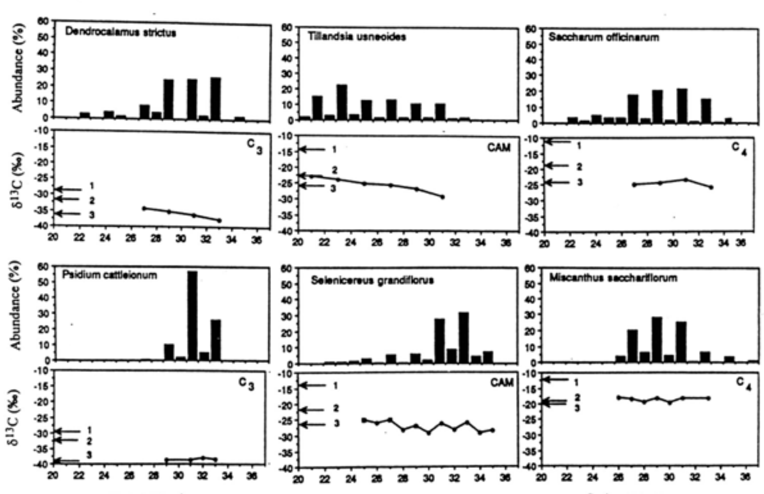

Fig. 1. Individual $\delta^{13}C$ values (‰ vs PDB) and relative abundances (% of total alkane fraction) vs *n*-alkane carbon number for plant waxes extracted from representative plants of different CO_2 metabolisms. 1, $\delta^{13}C$ value for leaf total tissue; 2, $\delta^{13}C$ value for total surface lipid extract; 3, weighted mean average $\delta^{13}C$ value for individual *n*-alkanes.

Influence of long-term degradation on isotopic composition of leaf-wax biomarker lipids

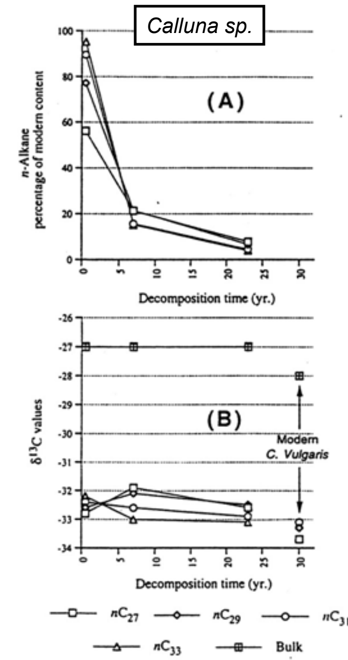

Long range transport and preservation of plant wax alkanes in marine sediments

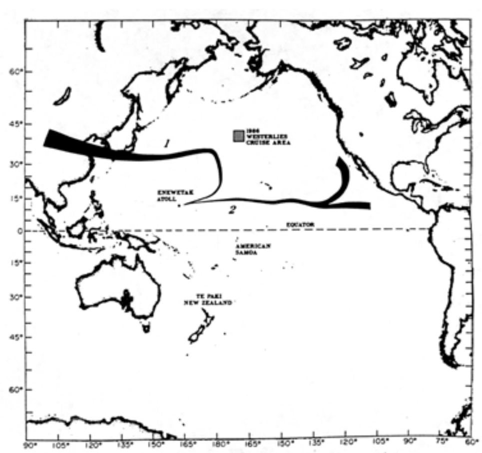

Fig. 1. Locations of the major SEAREX sampling sites and some of the typical air mass trajectories for the Enewetak site: (1) dry season; (2) wet season.

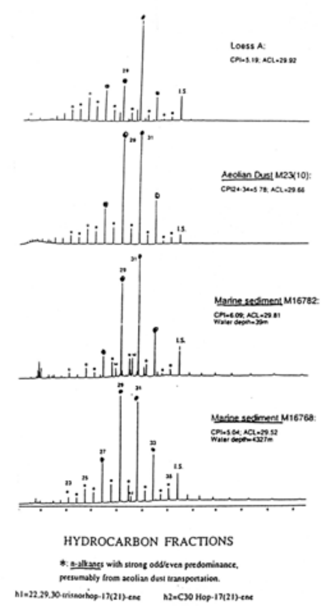

Gagosian and Peltzer

Eglinton (senior) et al

Vegetation zones of Africa (modern and past glacial)

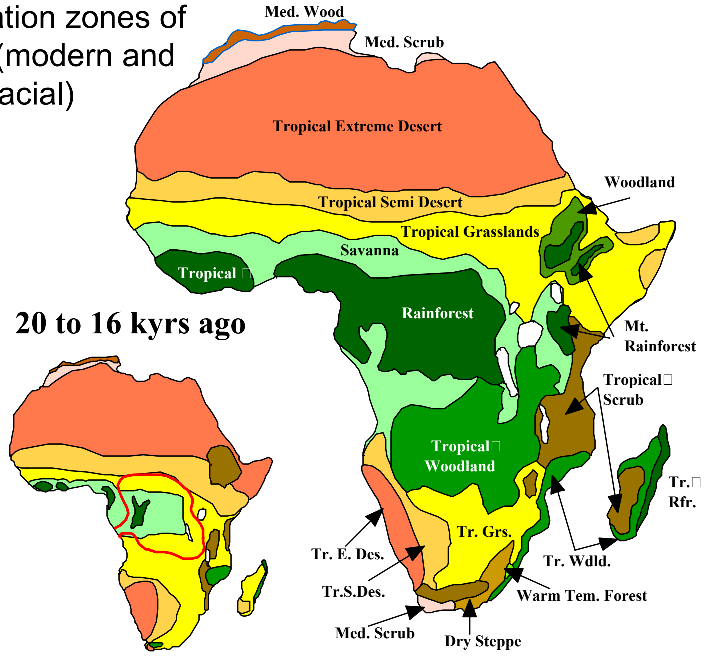

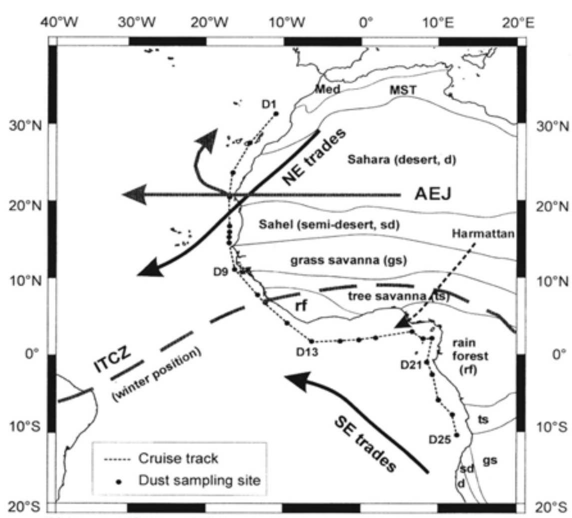

Fig. 1. Ship track and dust sampling sites of *RV Meteor* cruise M41/1 along the West African margin. Phytogeographical zonation of Africa is taken from White (1983): Med = Mediterranean vegetation; MST = Mediterranean–Saharan transition; d = desert; sd = semidesert; gs = grass savanna; ts = tree savanna; rf = rain forest. Major wind systems are drawn after Kalu (1979), Tetzlaff and Wolter (1980), and Sarnthein et al. (1981). Note that samples D19 and D20 were taken at almost the same location.

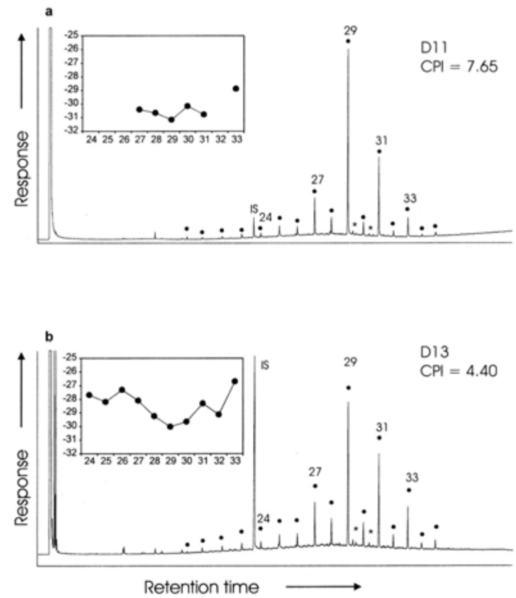

Fig. 3. Gas chromatographic traces of saturated hydrocarbon fractions of organic solvent extracts of aerosol samples with (a) a high and (b) a low CPI (above: D11, CPI = 7.65; below: D13, CPI = 4.40). Dots indicate *n*-alkanes, stars indicate $17\alpha,21\beta$(H)-hopanes. Insets show stable carbon isotopic compositions (in ‰) vs. chain-length of *n*-alkanes.

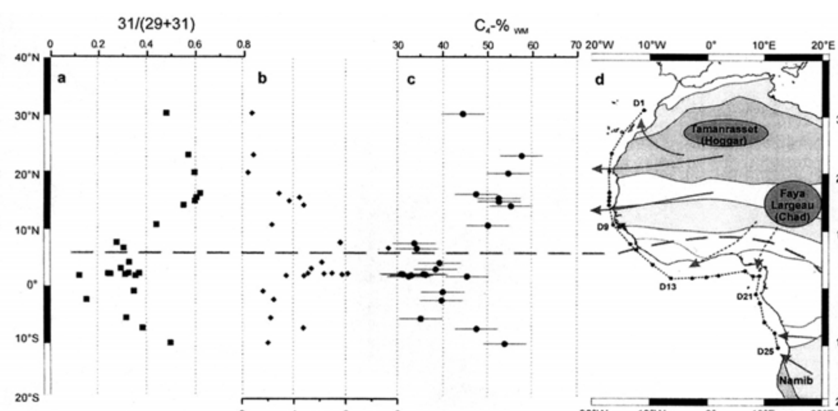

Fig. 4. (a) The variation in the ratio of the two dominant *n*-alkane homologues *n*-C_{31}/(*n*-C_{29} + *n*-C_{31}), (b) the CPI, and (c) the percentage of C_4 plant-derived *n*-alkanes in the aerosol samples vs. latitude. Ship track and sampling sites are shown. Note that sample D2 is missing. (d) Vegetation zones on the continent with mixed C_3/C_4 plant vegetation are light shaded, the Sahara and Namib desert with sparse but predominant C_4 plant vegetation are dark shaded. Major dust source regions and schematic transport pathways are indicated. The gray stippled line indicates the position of the ITCZ.

Plant wax (C_{29} *n*-alkane) carbon isotopes of African dust and E-Atlantic surface sediments

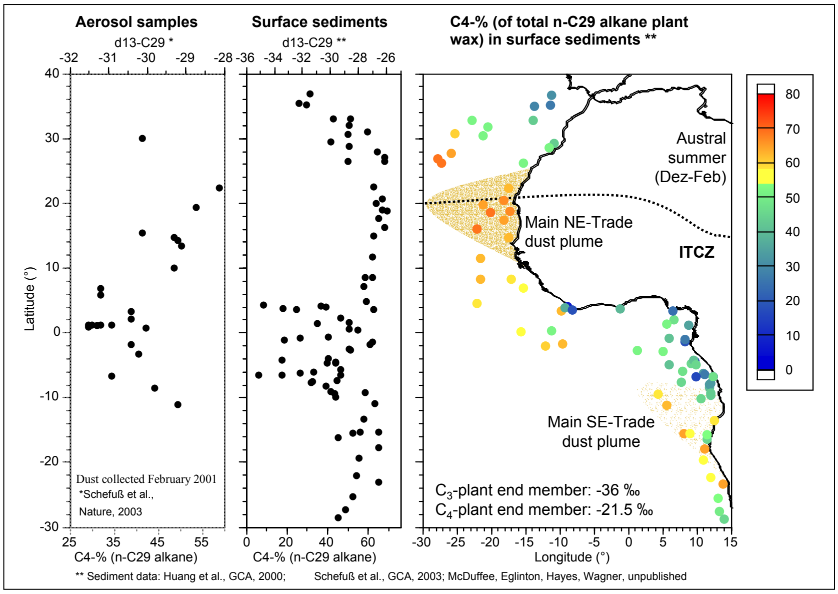

Carbon isotopic composition of dustfall sample off NW Africa

Fractions	Concn. (gdw basis)	$\delta^{13}C$ (‰)	$\Delta^{14}C$ (‰)	^{14}C age (yr BP)
Total Organic Carbon	1.02 %	-18.93	-149.6	1260 ± 40
Black Carbon	0.24 %	-15.13	-231.7	2070 ± 35
Plant wax alcohols	12 µg	-27.9	-80.8	649 ± 143

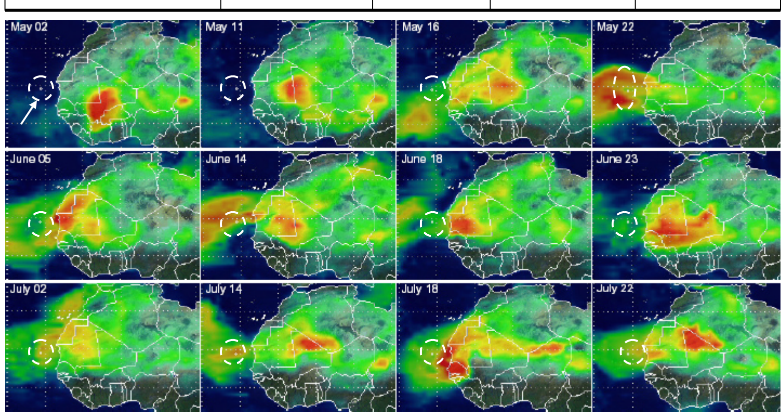

Eglinton et al., G^3, 2002

Isotopic compositions of Bengal fan sediments and the emergence of C4 plants

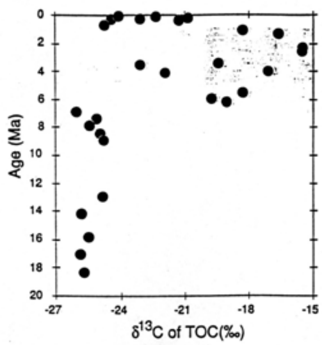

FIG. 2. $\delta^{13}C$ of TOC in Bengal Fan sediments plotted against age in Holes 717C and 718B. Data are available upon request to the authors or in NOAA data base. The increase of $\delta^{13}C$ values at *ca.* 7 Ma reflects the increase of the C4/C3 plant ratio in the source of the organic matter. The $\delta^{13}C$ increase near 7 Ma closely parallels that observed in paleosol studies in the Himalayan foreland (e.g., CERLING, et al., 1993), but the decrease after 0.9 Ma is not observed in the paleosol data. Variations in $\delta^{13}C$ are correlated with variations in sedimentation rate, grain size and clay mineralogy (Fig. 1).

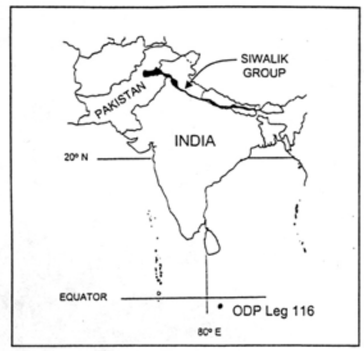

Fig. 1. Map of the Indian subcontinent showing outcrop pattern of Siwalik Group and sample localities for both paleosol and marine sediments (insert map).

Isotopic compositions of Bengal fan sediments and the emergence of C4 plants

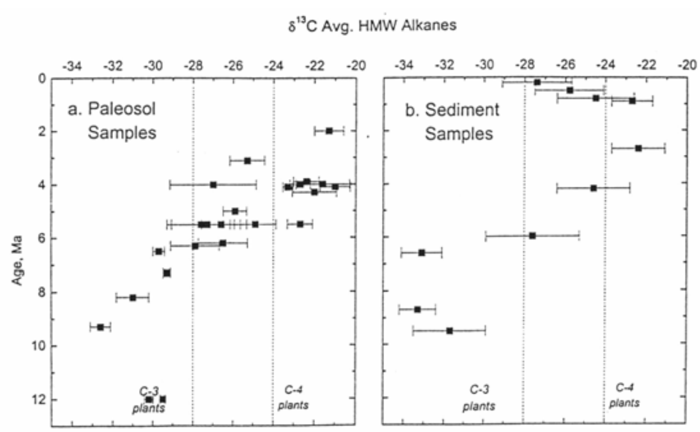

Fig. 6. $\delta^{13}C$ values representing the average of odd-carbon-numbered HMW alkanes plotted as a function of sample age for both the paleosol and sediment samples. Dotted line represent the approximate limits of *n*-alkane $\delta^{13}C$ values expected for C-3 and C-4 plants (see text and Table 14). Paleosol samples with evidence for significant contribution of *n*-alkanes from parent materials are not included.

^{14}C age of OC in marine sediment core-tops (0-3 cm)

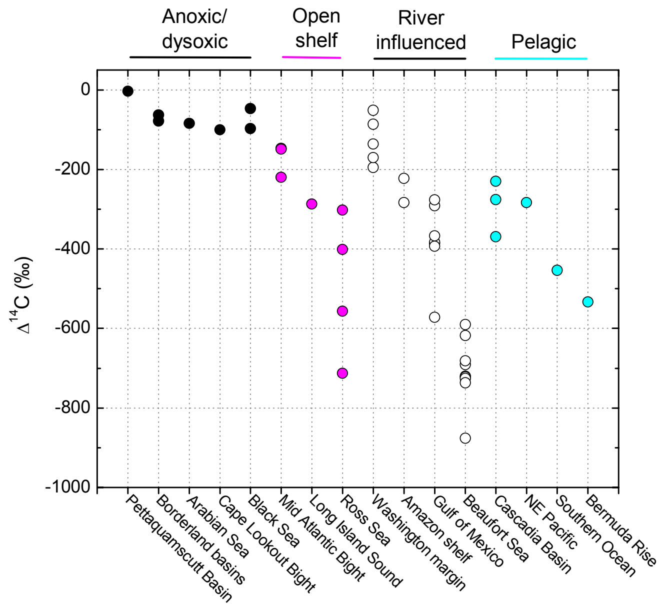

^{14}C variability in riverine suspended particulate organic matter

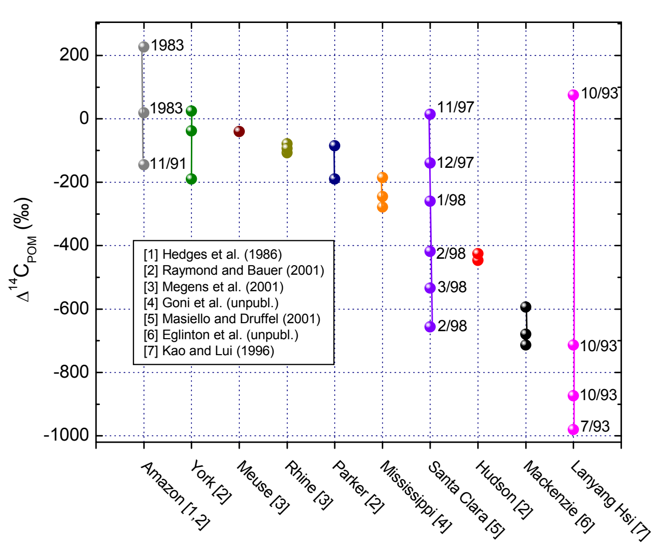

Importance of tropical mountainous river systems in terrigenous OC export to the oceans

Fig. 1 Annual discharge of total organic carbon of major world rivers to the oceans (organic carbon fluxes are in 10^{12} gC year^{-1}; wet tropics are underlain in *dark grey*). Data are from: Telang et al. (1991; Mackenzie, Yukon, St. Lawrence, Mississippi); Depetris and Paolini (1991; Orinoco, Parana); Richey et al. (1991; Amazon); Martins and Probst (1991; Zaire, Niger); Degens et al. (1991; Nile); Kempe et al. (1991; Rhine + Elbe, Seine + Loire + Gironde); Telang et al. (1991; Ob, Yenisei, Lena); Gan-Wei-Bin et al. (1983; Yangtze); Subramanian and Ittekkot (1991; Ganges + Brahmaputra + Indus); Bird et al. (1995; Oceania)

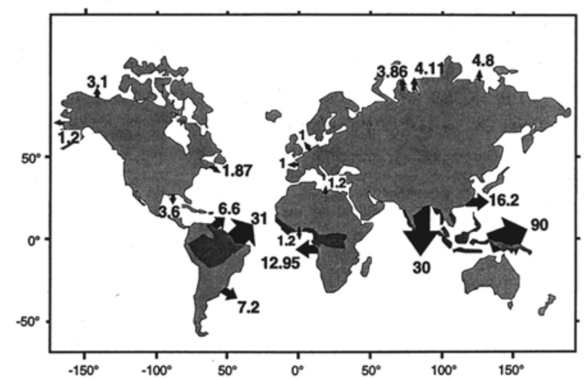

Milliman et al

Importance of tropical mountainous river systems in terrigenous OC export to the oceans

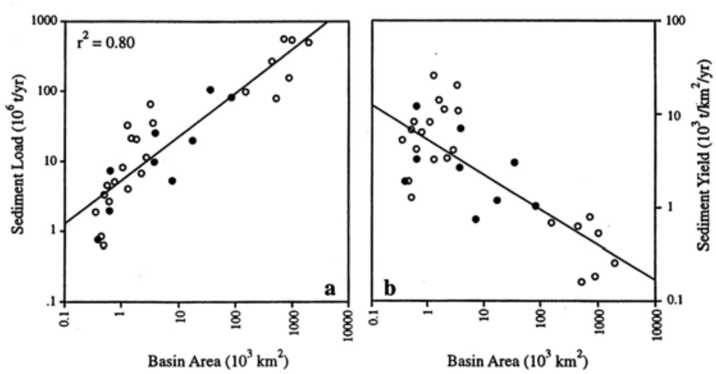

Fig. 1. Relationship between annual sediment load (a) and sediment yield (b) and basin area for various southeast Asian and Indonesian/Papua New Guinean humid (>500 mm y^{-1} run-off), mountain (>1000 m headwater elevation) rivers. Note that the East Indies rivers (Fly, Purari, Solo, Citamandy, Cimanuk, Cimuntur, Cilutung, Cijolang, and Agno; solid dots) have loads and yields very near values predicted based solely on southeast Asian river (open circles) algorithms; see text for further discussion. Data from Milliman and Syvitski (1992), somewhat modified by Milliman and Farnsworth (in prep.).

Terrigenous OC delivery and deposition on the Eel Margin

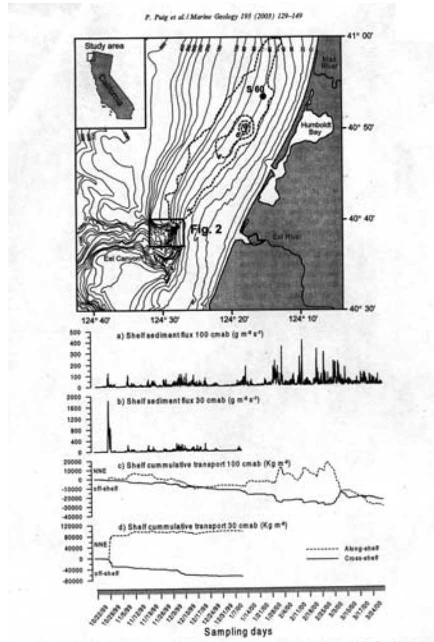

Fig. 8. Temporal evolution of the instantaneous suspended-sediment flux magnitude and cumulative suspended-sediment transport along-shelf and cross-shelf at the S-60 site during the entire study.

Terrigenous OC delivery and deposition on the Eel Margin

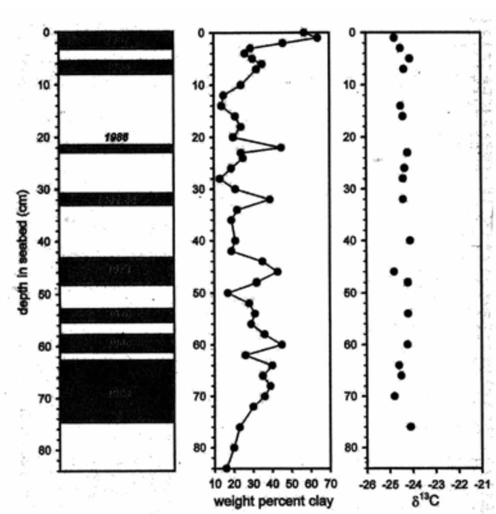

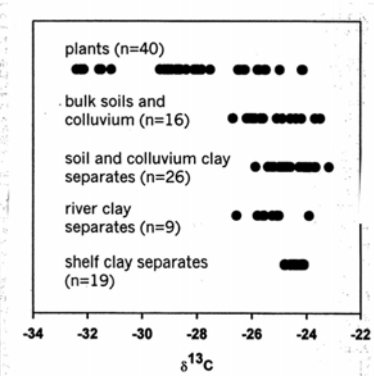

Fig. 6. Stable carbon isotopic composition of plants, soils, colluvium, and riverine suspensions in the Eel River watershed and of clay-sized sediment at the K70 site on the Eel River shelf. To date, we have been able to sample river suspensions only at flows of less than 3700 $m^3 s^{-1}$. The available data suggest that particles in transport at progressively higher discharges have more positive $\delta^{13}C$ values, a trend that we hypothesize reflects a greater contribution from mass wasting of melange vs. erosion of topsoil during more extreme precipitation events.

The Mackenzie/Beaufort System

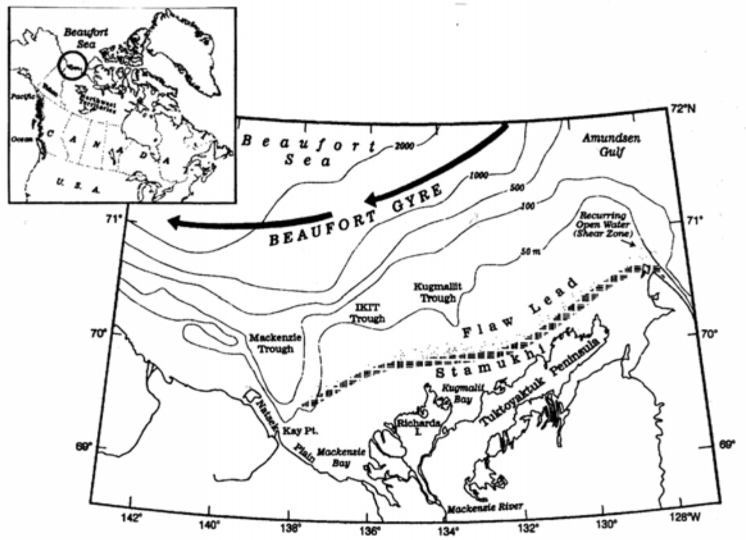

Fig. 1. Location map of the Mackenzie Shelf in the Canadian Beaufort Sea showing the various features discussed in the text.

Riverine delivery and transport of OC (Mackenzie/Beaufort)

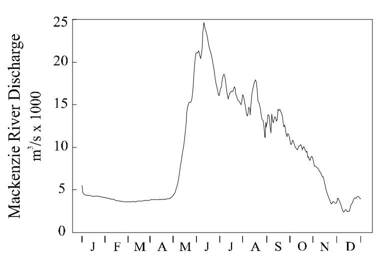

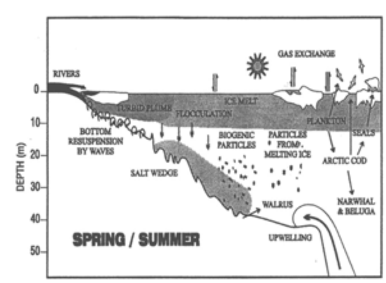

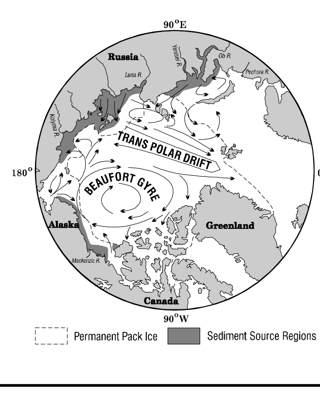

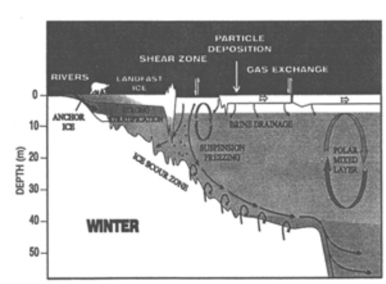

^{14}C ages of suspended particulate and sedimentary OC in river dominated systems

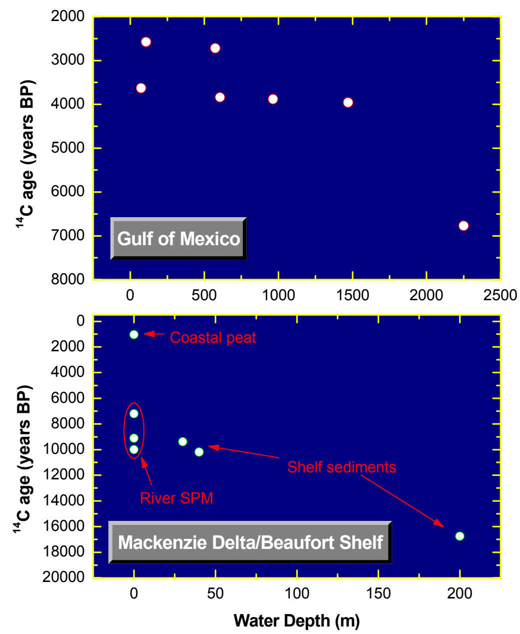

Geochemical Characteristics of OC in the Mackenzie/Beaufort system

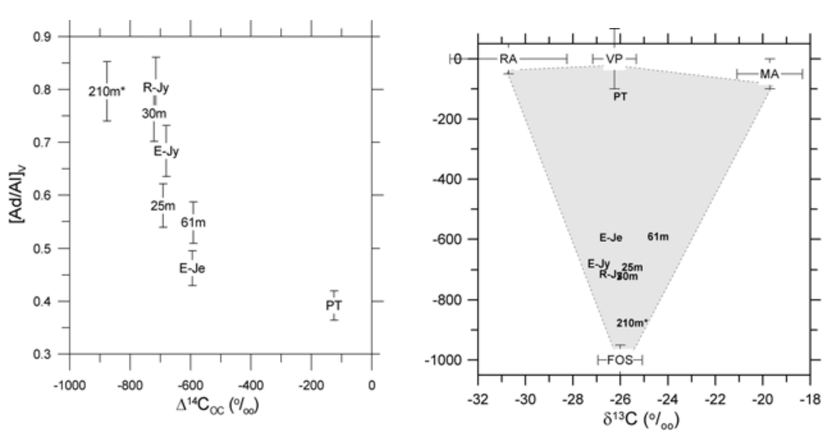

Goni et al. 2005